Available online at www.sciencedirect.com
SCIENCE DIRECT®
International Journal of Solids and Structures 42 (2005) 5208–5223
INTERNATIONAL JOURNAL OF SOLIDS and STRUCTURES
www.elsevier.com/locate/ijsolstr

Thermal stress intensity factors for a crack in an anisotropic half plane

L. Liu, G.A. Kardomateas *

Georgia Institute of Technology, School of Aerospace Engineering, Atlanta, GA 30332, United States

Received 19 June 2004; received in revised form 15 February 2005
Available online 7 April 2005

Abstract

On the basis of the two-dimensional theory of anisotropic thermoelasticity, a solution is given for the thermal stress intensity factors due to the obstruction of a uniform heat flux by an insulated line crack in a generally anisotropic half plane. The crack is replaced by continuous distributions of sources of temperature discontinuity and dislocations. First, the particular thermoelastic dislocation solutions for the half plane are obtained; then the corresponding isothermal solutions are superposed to satisfy the traction-free conditions on the crack surfaces. The dislocation solutions are applied to calculate the thermal stress intensity factors, which are validated by the exact solutions. The effects of the uniform heat flux, the ply angle and the crack length are investigated.

Keywords: Thermal; Crack; Heat flux; Anisotropic; Composite; Fracture; Stress intensity factors; Thermoelastic dislocation

1. Introduction

Composite materials are often subjected to the combined action of a mechanical loading and a thermal loading, for example in instances of fire. Defects that are unavoidable and characteristic for many structures decrease their strength and life. The accurate stress intensity-factor evaluation is essential in the prediction of failure and the calculation of crack growth rate in these structures. A number of plane thermoelastic boundary-value problems have been solved for a generally anisotropic material using the Fourier integral transform technique. For example, using the basic equations derived by Clements (1973) for anisotropic thermoelasticity, Clements and Toy (1976) considered two thermoelastic contact problems; Following their work, Atkinson and Clements (1997) gave a solution of the two-dimensional

* Corresponding author. Tel.: +1 404 894 8198; fax: +1 404 894 2760.
E-mail address: george.kardomateas@aerospace.gatech.edu (G.A. Kardomateas).

0020-7683/$ - see front matter © 2005 Elsevier Ltd. All rights reserved.
doi:10.1016/j.ijsolstr.2005.02.025

Griffith crack obstructing a uniform heat flux. Using the techniques of Fourier transforms and multiple integrations, Tsai (1983, 1984) studied the crack embedded in a transversely isotropic or orthotropic material. However, we note that it is not easy for the Fourier transform method to give explicit expressions for the stresses and displacements. It also requires to pay very careful attention to the way the representation behaves at infinity to avoid possible divergent integrals. Sturla and Barber (1988a,b) reconsidered the two-dimensional Griffith crack problem in an infinite medium by the Green function formulation and expressed the thermal stress distribution and stress intensity factors in terms of physical variables. They gave the exact solution for the crack problem in an infinite medium. But, again, it is not an easy task to derive the Green's function for more complex boundary-value problems such as the half plane (considered here), the strip or bi-material configurations with complicated heat flux or temperature field distribution.

A alternative and very effective method to study crack problems, which has been extensively used in isothermal anisotropic problems is the continuous dislocation technique. Eshelby et al. (1953) and Stroh (1958) presented analytical solutions for a single dislocation in a generally anisotropic medium. Following their work, Ting (1986), Atkinson and Eftaxiopoulos (1991), Civelek and Erdogan (1982), Suo (1990), Suo and Hutchinson (1990) and Huang and Kardomateas (2001) considered various isothermal crack problems involving anisotropic infinite plane, half plane, strip and bi-material problems. Sekine (1977) used continuous distributions of sources of temperature discontinuity and edge dislocations to model the insulated line crack along an arbitrary direction under uniform heat flux, in order to solve the thermoelastic problem in an isotropic half plane. To the author's knowledge, however very little work have been done for generally anisotropic thermoelastic problems using the technique (and none for the anisotropic half plane which is considered herewith).

In this paper, we used the basic formulations derived by Clements (1973) and Sturla and Barber (1988b) plus appropriate image systems to get zero heat flow along a free boundary. The particular thermoelastic solution is superposed with the corresponding isothermal solution in order to get zero traction along the free boundary. The analytic solution for a single dislocation is presented firstly, then the crack is replaced by a distribution of such dislocations and a system of singular integral equations is formulated. To solve the system, we use the inversion theorem for Cauchy integral equations and turn them to a set of Fredholm integral equations of the second kind, which is solved by a standard numerical method. Having obtained the dislocation densities, we can appropriately obtain the mixed-mode thermal stress intensity factors. Some results of practical interest are presented.

2. Formulation

Let x_1, x_2, x_3 denote Cartesian coordinates and consider a homogeneous generally anisotropic half plane with a crack parallel to the free boundary $x_2 = 0$ under a uniform heat flow, as shown in Fig. 1. The crack is assumed to be fully open, hence be traction-free and to prevent the transfer of heat between its faces. The corresponding boundary conditions are:

$$q_2 = 0; \quad -a < x_1 < +a; \ \ x_2 = x_{20}, \tag{2.1}$$

$$\sigma_{i2} = 0; \quad -a < x_1 < +a; \ \ x_2 = x_{20}, \tag{2.2}$$

$$q_2 = q_0; \quad -\infty < x_1 < +\infty; \ \ x_2 = 0, \tag{2.3}$$

$$\sigma_{i2} = 0; \quad -\infty < x_1 < +\infty; \ \ x_2 = 0, \tag{2.4}$$

$$q_2 = q_0; \quad \sqrt{x_1^2 + x_2^2} \to \infty, \tag{2.5}$$

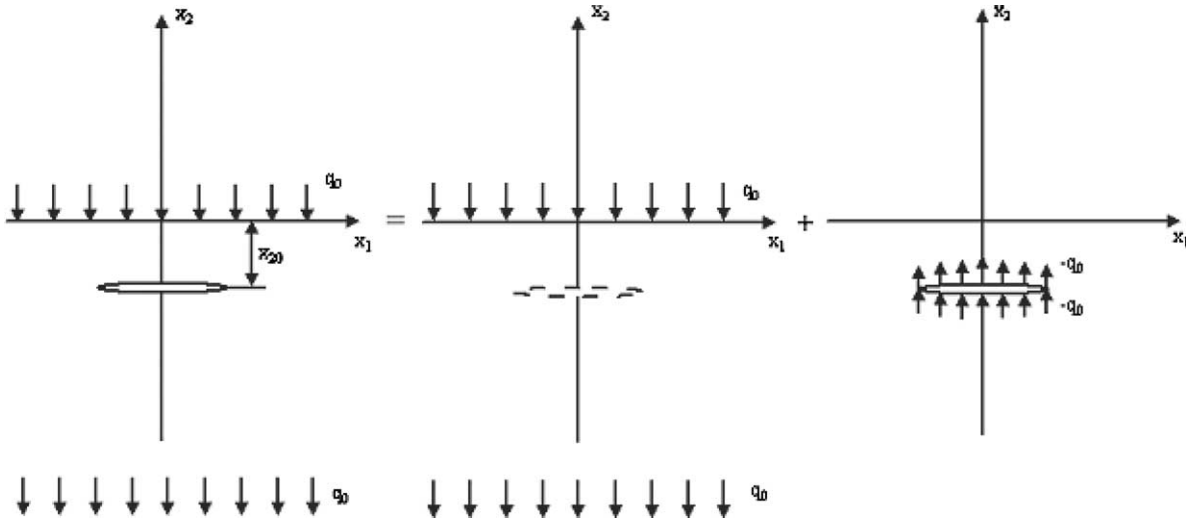

Fig. 1. The thermoelastic fully-open crack in half plane.

$$\sigma_{ij} = 0; \qquad \sqrt{x_1^2 + x_2^2} \to \infty. \tag{2.6}$$

The configuration can be decomposed into two parts (Fig. 1); the first is the configuration without the crack under uniform heat flow, which involves no thermal stress; the second is the corrective configuration, for which the boundary conditions are:

$$q_2 = -q_0; \quad -a < x_1 < +a; \ \ x_2 = x_{20}, \tag{2.7}$$

$$\sigma_{i2} = 0; \quad -a < x_1 < +a; \ \ x_2 = x_{20}, \tag{2.8}$$

$$q_2 = 0; \quad -\infty < x_1 < +\infty; \ \ x_2 = 0, \tag{2.9}$$

$$\sigma_{i2} = 0; \quad -\infty < x_1 < +\infty; \ \ x_2 = 0, \tag{2.10}$$

$$q_2 = 0; \quad \sqrt{x_1^2 + x_2^2} \to \infty, \tag{2.11}$$

$$\sigma_{ij} = 0; \quad \sqrt{x_1^2 + x_2^2} \to \infty. \tag{2.12}$$

2.1. A single dislocation in a half plane

2.1.1. The temperature field for a single dislocation in a half plane

We present here the solution for a single dislocation in a half plane configuration. A dislocation, with the temperature discontinuity strength and Burgers vector b_i emerges at the point (x_{10}, x_{20}), which is shown in Fig. 2.

The relation between the heat flux, q_i, and the temperature, T, is given by:

$$q_i = -k_{ij} \frac{\partial T}{\partial x_j}, \tag{2.1.1}$$

where $i,j = 1,2,3$, and k_{ij} are the thermal conductivity constants and $k_{ij} = k_{ji}$.

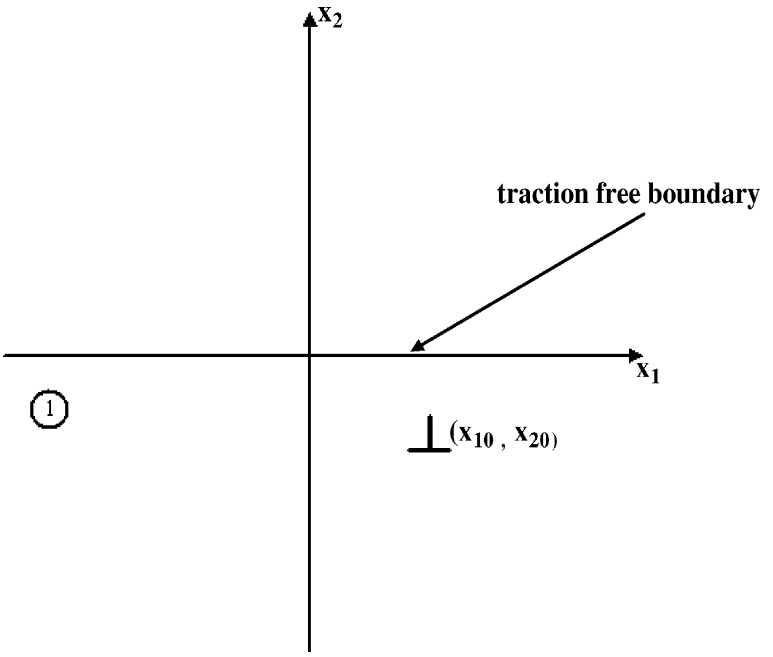

Fig. 2. A dislocation near the free boundary.

The temperature must satisfy the heat conduction equation:

$$k_{ij}\frac{\partial^2 T}{\partial x_i \partial x_j} = 0, \tag{2.1.2}$$

and this is satisfied by:

$$T(x_1, x_2) = f(x_1 + \tau x_2) + \bar{f}(x_1 + \bar{\tau} x_2), \tag{2.1.3}$$

where τ is the heat eigenvalue and it is the root with positive imaginary part of the equation:

$$k_{11} + 2k_{12}\tau + k_{22}\tau^2 = 0. \tag{2.1.4}$$

Then, the temperature field can be written as:

$$T(x_1, x_2) = f(z_t) + \bar{f}(\bar{z}_t), \tag{2.1.5}$$

where $z_t = x_1 + \tau x_2$ and $f(z_t)$ is any analytical function of z_t.

If $\phi(z_t)$ is any function of x_1 and x_2, the heat flux in the form:

$$q_1 = -\frac{\partial \phi}{\partial x_2}; \qquad q_2 = \frac{\partial \phi}{\partial x_1}, \tag{2.1.6}$$

satisfy Eq. (2.1.2) identically. Eqs. (2.1.3), (2.1.5) and (2.1.6) give:

$$\phi(x_1, x_2) = l_t f(z_t) + \bar{l}_t \bar{f}(\bar{z}_t), \tag{2.1.7}$$

thus

$$q_1 = -l_t \tau f'(z_t) - \bar{l}_t \bar{\tau} \bar{f}'(\bar{z}_t), \tag{2.1.8a}$$

$$q_2 = l_t f'(z_t) + \bar{l}_t \bar{f}'(\bar{z}_t), \tag{2.1.8b}$$

where

$$l_t = -k_{12} - \tau k_{22}. \tag{2.1.9}$$

Let us introduce a constant m_t, defined by:

$$l_t m_t = 1. \tag{2.1.10}$$

All of the above, concerned with an infinite plane configuration, can also be implemented in the case of a medium with a heat flux free boundary, but we shall have to choose the function $f(z_t)$ such that:

$$q_2(x_1, 0) = 0. \tag{2.1.11}$$

For this purpose, a function is chosen first for the temperature field due to a single dislocation in an infinite medium:

$$v(z_t) = \frac{1}{4\pi} m_t d_t \log(z_t - \xi_t), \tag{2.1.12}$$

where

$$\xi_t = x_{10} + \tau x_{20}, \tag{2.1.13}$$

$$t = B_t d_t, \tag{2.1.14}$$

$$B_t = \frac{\mathrm{i}}{2}(m_t - \bar{m}_t), \tag{2.1.15}$$

where t represents the temperature discontinuity strength.

It can be proved that d_t is real, as follows. From Eqs. (2.1.12) and (2.1.7), we obtain:

$$\phi(x_1, x_2) = l_t \frac{1}{4\pi} m_t d_t \log(z_t - \xi_t) + \bar{l}_t \frac{1}{4\pi} \bar{m}_t \bar{d}_t \log(z_t - \xi_t) = \frac{1}{4\pi} d_t \log(z_t - \xi_t) + \frac{1}{4\pi} \bar{d}_t \log(z_t - \xi_t).$$

The change in ϕ along a closed path about the point ξ_t is:

$$\Delta\phi = 2\pi\mathrm{i}\left(\frac{1}{4\pi} d_t - \frac{1}{4\pi} \bar{d}_t\right) = \frac{\mathrm{i}}{2}(d_t - \bar{d}_t).$$

This change in ϕ represents the next heat source at that point ξ_t. In order to have a pure temperature discontinuity without a net heat source, it is clear that $\Delta\phi = 0$, therefore d_t is real.

Furthermore, since B_t is also real, it is clear from Eq. (2.1.14) that t is real as well.

Now, another function, $w(z_t)$, has to be found to ensure the free heat flux boundary condition at the axis $x_2 = 0$, so that when added to $v(z_t)$, then

$$f(z_t) = v(z_t) + w(z_t). \tag{2.1.16}$$

Therefore, we require:

$$\frac{1}{4\pi} l_t m_t d_t \frac{1}{x_1 - \xi_t} + \bar{l}_t \bar{w}_t'(x_1) = 0 \tag{2.1.17}$$

or,

$$w'(x_1) = -\frac{1}{4\pi} m_t d_t \frac{1}{x_1 - \bar{\xi}_t}. \tag{2.1.18}$$

Finally, we obtain:

$$w(z_t) = -\frac{1}{4\pi} m_t d_t \log(z_t - \bar{\xi}_t), \tag{2.1.19}$$

then

$$f(z_t) = \frac{1}{4\pi} m_t d_t \log(z_t - \xi_t) - \frac{1}{4\pi} m_t d_t \log(z_t - \bar{\xi}_t). \tag{2.1.20}$$

The first part of Eq. (2.1.20) represents the temperature distribution due to a single dislocation in an infinite plane, the second part represents the boundary influence on the temperature field, it also can be seen as an appropriate image dislocation located at the point $\bar{\xi}_t(x_{10}, -x_{20})$ in the infinite plane. Due to the symmetric distribution of the two dislocations, the heat flux at the symmetry axis $x_2 = 0$ equals to zero.

2.1.2. The stress field for a single dislocation in a half plane

A particular thermoelastic solution for a single dislocation at the position $\xi(x_{10}, x_{20})$ in an infinite plane can be written as (Sturla and Barber, 1988a,b)

$$\sigma_{i2} = Q_i \left[\frac{1}{4\pi} m_t d_t \log|z_t - \xi_t| \right] + \text{CC}, \tag{2.1.21}$$

where CC denotes the complex conjugate and Q_i is defined by the material constants. Also, $i = 1, 2, 3$ and the variables with subscript t refer to the scalars associated with the temperature field. For the infinite plane configuration, the traction due to the single dislocation at $\xi(x_{10}, x_{20})$ is given by Eq. (2.1.21). As for the influence of the free heat flux boundary, the traction due to the image dislocation at the symmetric position $\bar{\xi}_t(x_{10}, -x_{20})$ is given by Eq. (2.1.21) as well. Finally, we obtain the particular thermoelastic solution in the half plane configuration

$$\sigma_{i2} = Q_i \left[\frac{1}{4\pi} m_t d_t (\log|z_t - \xi_t| - \log|z_t - \bar{\xi}_t|) \right] + \text{CC}. \tag{2.1.22}$$

For the half plane configuration, the traction free boundary condition

$$\sigma_{i2}(x_1, 0) = 0, \tag{2.1.23}$$

should be satisfied as well, so an isothermal solution should be superposed to ensure the traction free boundary condition.

To solve the problem, we make use of the basic formulations from Stroh (1958), in which the displacement is written as (in the following equations, $i, k, \alpha = 1, 2, 3$):

$$u_k = \sum_\alpha A_{k\alpha} \varphi_\alpha(z_\alpha) + \sum_\alpha \overline{A}_{k\alpha} \bar{\varphi}_\alpha(\bar{z}_\alpha), \tag{2.1.24}$$

where

$$z_\alpha = x_1 + p_\alpha x_2, \tag{2.1.25}$$

and the p_α are the three roots with positive imaginary part of the equation

$$\left| c_{i1k1} + p_\alpha (c_{i1k2} + c_{i2k1}) + p_\alpha^2 c_{i2k2} \right| = 0, \tag{2.1.26}$$

c_{ijkl} are the elastic constants and the stress components σ_{ij} are defined in terms of the function:

$$\Omega_i = \sum_\alpha L_{i\alpha} \varphi_\alpha(z_\alpha) + \sum_\alpha \overline{L}_{i\alpha} \bar{\varphi}_\alpha(\bar{z}_\alpha), \tag{2.1.27}$$

where

$$L_{i\alpha} = (c_{i2k1} + p_\alpha c_{i2k2}) A_{k\alpha}. \tag{2.1.28}$$

In particular, we have

$$\sigma_{i2} = \sum_\alpha L_{i\alpha} \varphi'_\alpha(z_\alpha) + \sum_\alpha \overline{L}_{i\alpha} \bar{\varphi}'_\alpha(\bar{z}_\alpha), \tag{2.1.29}$$

so, we require:

$$\sum_\alpha L_{i\alpha} \varphi'_\alpha(x_1) + \sum_\alpha \overline{L}_{i\alpha} \bar{\varphi}'_\alpha(x_1) + \frac{1}{4\pi} Q_i m_t d_t [\log(x_1 - \xi_t) - \log(x_1 - \bar{\xi}_t)] + \frac{1}{4\pi} \overline{Q}_i \bar{m}_t d_t [\log(x_1 - \bar{\xi}_t) - \log(x_1 - \xi_t)] = 0. \tag{2.1.30}$$

This results in:

$$\overline{L}_{i\alpha} \bar{\varphi}'_\alpha(x_1) + \frac{1}{4\pi} Q_i [m_t d_t \log(x_1 - \xi_t)] - \frac{1}{4\pi} \overline{Q}_i [\bar{m}_t d_t \log(x_1 - \xi_t)] = 0. \tag{2.1.31}$$

Finally, we obtain:

$$\varphi'_\alpha(z_\alpha) = \frac{1}{4\pi} M_{\alpha i} (Q_i m_t d_t - \overline{Q}_i \bar{m}_t d_t) \log(z_\alpha - \bar{\xi}_t). \tag{2.1.32}$$

In the latter equation, the relationship between $L_{\alpha i}$ and $M_{\alpha i}$ is (for detailed explanation, refer to Stroh, 1958):

$$M_{\alpha i} L_{i\beta} = \delta_{\alpha\beta}.$$

So, the required particular thermoelastic solution now can be obtained by superposing the particular solution of Eq. (2.1.22) and the general isothermal solution of Eqs. (2.1.29) and (2.1.32). In particular, we find the stress σ_{i2} is given by:

$$\sigma_{i2} = 2\,\mathrm{Re}\left\{ \frac{1}{4\pi} Q_i m_t d_t \left[\log(z_t - \xi_t) - \log(z_t - \bar{\xi}_t) \right] + \frac{1}{4\pi} L_{i\alpha} \left[M_{\alpha k} (Q_k m_t d_t - \overline{Q}_k \bar{m}_t d_t) \log(z_\alpha - \bar{\xi}_t) \right] \right\}, \tag{2.1.33}$$

where Re means the real part of the complex function.

2.2. A fully-open crack in an anisotropic half plane as a series of dislocations

Consider a fully open crack of length $2a$ parallel to the free boundary under uniform heat flux in an anisotropic half plane (configuration shown in Fig. 1). The temperature, T, and heat flux, q_i, distribution with a single dislocation for a half plane configuration can be determined by Eqs. (2.1.5), (2.1.8) and (2.1.20).

Now, the crack is replaced by a series of dislocations with the temperature discontinuity strength t at each dislocation point. Then, we have:

$$q_2(x_1, x_{20}) = \int_{-a}^{+a} \tilde{q}_2(x_1, x_{20}, s, x_{20}) t(s, x_{20})\, \mathrm{d}s = -q_0(x_1, x_{20}), \tag{2.2.1}$$

where $\tilde{q}_2(x_1, x_{20}, s, x_{20})$ represents the heat flux at the point (x_1, x_{20}) due to the dislocation with unit temperature discontinuity strength at the point (s, x_{20}), so it can be determined by Eqs. (2.1.8b) and (2.1.20) by

setting $t = 1$. In order to satisfy the boundary condition Eq. (2.7), Eq. (2.2.1) should equal to the opposite of the external heat flux q_0.

Eq. (2.2.1) is a singular integral equation with the typical Cauchy kernel; it can be transformed into $N-1$ linear algebraic equations by the case I Gaussian formulas following Hills et al. (1996)

$$\pi a \tilde{q}_2(x_{1,k}, x_{20}, s_m, x_{20}) W_m \tilde{t}(\tilde{s}_m, x_{20}) = -q_0(x_{1,k}, x_{20}), \tag{2.2.2}$$

where $k = 1, 2, \ldots, N-1$; $m = 1, 2, \ldots, N$ and N is the number of integration points. Also, s_m are integration points, $x_{1,k}$ are collocation points and W_i are the weight functions appropriate to the quadrature formula employed; they are given by:

$$s_m = a\tilde{s}_m; \qquad x_{1,k} = a\tilde{t}_k; \qquad \tilde{t}(\tilde{s}_m, x_{20}) = \frac{t(\tilde{s}_m, x_{20})}{\sqrt{1-\tilde{s}_m^2}}; \tag{2.2.3}$$

$$\tilde{s}_m = \cos\left[\frac{\pi(2m-1)}{2N}\right]; \qquad \tilde{t}_k = \cos\left[\pi\left(\frac{k}{N}\right)\right]; \qquad W_m = \frac{1}{N}. \tag{2.2.4}$$

The temperature continuity outside the crack can be imposed by enforcing the auxiliary condition:

$$\sum_{m=1}^{N} W_m \tilde{t}(\tilde{s}_m, x_{20}) = 0. \tag{2.2.5}$$

Following Eqs. (2.2.2) and (2.2.5), the temperature discontinuity strength $\tilde{t}$ at each integration point $(\tilde{s}_m, x_{20})$ can be determined.

The particular thermoelastic traction along the crack surfaces is associated with the temperature discontinuity strength at each integration point, which can be written as:

$$\sigma_{ij}^p(x_1, x_2) = \int_{-a}^{+a} \tilde{\sigma}_{ij}^p(x_1, x_2, s, x_{20})\,\mathrm{d}s, \quad ij = 21, 22, 23, \tag{2.2.6}$$

where $\tilde{\sigma}_{ij}(x_1, x_2, s, x_{20})$ represents the particular thermoelastic stress at the point (x_1, x_2) due to the temperature discontinuity strength at the point (s, x_{20}). If $t(s)$ is given, we can solve Eq. (2.2.6) by the standard numerical method. It has a *Generalized Cauchy kernel*, i.e. $\sigma_{ij}^p(x_1, x_{20}, s, x_{20})$ becomes unbounded as both the integration and collocation variables, s and x_1, tend to the same end-point. Since the temperature discontinuity strength function $t(s)$ is singular at each end-point, we can reduce Eq. (2.2.6) to a system of algebraic equations (Hills et al., 1996):

$$\sigma_{ij}^p(x_{1,k}, x_{20}) = \sum_{m=1}^{N} \tilde{\sigma}_{ij}^p(x_{1,k}, x_{20}, s_m, x_{20}), \tag{2.2.7}$$

where $\tilde{\sigma}_{ij}^p(x_{1,k}, x_{20}, s_m, x_{20})$ represents the stress at collocation point $(x_{1,k}, x_{20})$ due to the temperature discontinuity strength at the integration point (s_m, x_{20}). So Eq. (2.2.7) can be evaluated from Eq. (2.1.33) by substituting the temperature discontinuity strength at the N integration points.

To satisfy the traction-free boundary condition at the crack surfaces, we superpose a solution of the corresponding isothermal problem with traction equal and opposite to those of Eq. (2.2.7). This solution is conveniently represented by a distribution of dislocations of strength $b_i(s)$. The solution with a single dislocation $b_i(s)$ for an anisotropic half plane is given (Atkinson and Eftaxiopoulos, 1991). In particular, the stress σ_{i2} being:

$$\sigma_{i2} = \sum_{\alpha} L_{i\alpha} f'_{\alpha}(z_{\alpha}) + \sum_{\alpha} \overline{L}_{i\alpha} \overline{f}'_{\alpha}(\bar{z}_{\alpha}), \tag{2.2.8}$$

where

$$f(z_{\alpha}) = \frac{1}{4\pi} M_{\alpha j} d_j \log(z_{\alpha} - \xi_{\alpha}) - \frac{1}{4\pi} \sum_{\gamma} M_{\alpha k} \overline{L}_{k\gamma} \overline{M}_{\gamma j} d_j \log(z_{\alpha} - \bar{\xi}_{\gamma}), \tag{2.2.9}$$

$$b_i = B_{ij} d_j, \tag{2.2.10}$$

$$B_{ij} = \frac{\mathrm{i}}{2} (A_{i\alpha} M_{\alpha j} - \overline{A}_{i\alpha} \overline{M}_{\alpha j}). \tag{2.2.11}$$

Thus, the crack can be modeled as a series of dislocations with the densities $b_i(s, x_{20})$. The corresponding tractions along the crack surfaces due to the dislocation series are:

$$\sigma^{g}_{ij}(x_1, x_{20}) = \int_{-a}^{+a} \widetilde{F}_{ij}(x_1, x_{20}, s, x_{20}) b_i(s, x_{20})\, \mathrm{d}s, \quad ij = 21, 22, 23, \tag{2.2.12}$$

which should equal to the particular thermoelastic solution along the crack surfaces. In the previous expression, $\widetilde{\mathbf{F}}(x_1, x_{20}, s, x_{20})$ represents the stress at the point (x_1, x_{20}) due to the unit dislocation density $\mathbf{b}(s, x_{20})$, it can be obtained by Eq. (2.2.8) and (2.2.9) by setting $\mathbf{b} = \{1, 0, 0\}$, $\mathbf{b} = \{0, 1, 0\}$ and $\mathbf{b} = \{0, 0, 1\}$ respectively. We use the case I Gaussian formulas (Hills et al., 1996) to solve Eq. (2.2.12), which can be transformed to $3(N-1)$ linear algebraic equations:

$$\pi a \widetilde{F}_{ij}(x_{1,k}, x_{20}, s_m, x_{20}) \langle\langle W_m, W_m, W_m \rangle\rangle \tilde{b}_i(\tilde{s}_m, x_{20}) = -\sigma^{p}_{ij}(x_{1,k}, x_{20}), \tag{2.2.13}$$

where $x_{1,k}$, s_m, W_m are given by Eqs. (2.2.3) and (2.2.4) and:

$$\tilde{\mathbf{b}}(\tilde{s}_m, x_{20}) = \frac{\mathbf{b}(\tilde{s}_m, x_{20})}{\sqrt{1 - \tilde{s}_m^2}}. \tag{2.2.14}$$

In addition, it is also necessary to impose the closure condition, therefore three additional equations are obtained:

$$\sum_{m=1}^{N} W_m \tilde{b}_l(\tilde{s}_m, x_{20}) = 0; \quad l = 1, 2, 3. \tag{2.2.15}$$

Eqs. (2.2.13) and (2.2.15) enable us to calculate the dislocation densities $\tilde{\mathbf{b}}(\tilde{s}_m, x_{20})$ at the N integration points. The crack tip dislocation density can be extrapolated from the N integration points as (Hills et al., 1996):

$$\tilde{b}_l(1) = M_E \sum_{m=1}^{N} b_E(+1) \tilde{b}_l(\tilde{s}_m), \tag{2.2.16}$$

$$\tilde{b}_l(-1) = M_E \sum_{m=1}^{N} b_E(-1) \tilde{b}_l(\tilde{s}_{N+1-m}), \tag{2.2.17}$$

where

$$b_E(+1) = \sin\left[\frac{2m-1}{4N}\pi(2N-1)\right] \Big/ \sin\left(\frac{2m-1}{4N}\pi\right); \qquad b_E(-1) = b_E(+1); \qquad M_E = \frac{1}{N}. \tag{2.2.18}$$

The stress intensity factors at the crack tip can be calculated as (Huang and Kardomateas, 2001):

$$K_i(+1) = \frac{\sqrt{\pi a}}{2}\mathrm{Re}\left[L_{i\alpha}M_{\alpha j}B^{-1}_{j\gamma}\tilde{b}_\gamma(+1)\right], \tag{2.2.19}$$

$$K_i(-1) = -\frac{\sqrt{\pi a}}{2}\mathrm{Re}\left[L_{i\alpha}M_{\alpha j}B^{-1}_{j\gamma}\tilde{b}_\gamma(-1)\right], \tag{2.2.20}$$

where Re[·] stands for the real part of a complex variable and $\tilde{b}_\gamma(\pm 1)$ are solved from Eqs. (2.2.16) and (2.2.17).

3. Results and discussion

First, to validate the method, we choose the traction free boundary infinite; under this condition, the half plane solution should reduce to the solution for infinite plane. In this manner, it is easy to verify the solution because the analytical solution for the thermal stress intensity factors is known (Sturla and Barber, 1988b). The elastic material constants were taken from Kim et al. (2002) and listed in Table 1; x_1 is the laminate's longitudinal direction; x_2 is the normal direction (thicknesswise) of the lamina and the x_3 direction is determined by right-hand rule. The fiber orientation $\theta°$ is defined as the angle of the fibers with the x_1.

First, the convergence for the numerical integration is checked and the results are listed in Table 2. A 0° lamina is used in the calculation. The free boundary is located at $x_{20} = 5$ and the length of the crack $a = 1$. Obviously, as the number of integration points increases, the results of the thermal stress intensity factors converge well. In Fig. 3, we also show the convergence of the results with the number of integration points. In this figure, and all of the following figures, the SIFs are normalized with the Mode II stress intensity factor for an infinite plane and a zero deg. material, $K_{\mathrm{II}0}$, with a heat flux loading of $q = 1.0$ W/m K and a crack length $a = 1.0$ mm.

In order to validate the method, we set the free boundary at infinity. Thus, the half plane solution reduces to the solution of an infinite plane. In this manner, it is easy to verify the solution because the analytical solution for the thermal stress intensity factors in an infinite plane is known Sturla and Barber (1988a,b). Table 3 gives the comparison of the present solution for the limiting case of an infinite plane. The material is chosen to be 0°, 45° and 90° respectively. We assume the free boundary located at $x_{20} = 1.0 \times 10^9$ (a very large distance in order to simulate infinity). The dislocation results from this limiting case of the half plane compare well with the analytical solutions of the infinite plane. The agreement verifies the numerical method.

Next, we study the influence of the external heat flux to the mixed-mode thermal stress intensity factors. Figs. 4a, b and c give the Mode II, I and III SIFs for cracks in a half plane with different material choices as a function of the external heat flux. The crack is located at $x_{20} = -10$ and the length of the crack is $a = 1$. Fig. 4d and e give the Mode-II and Mode-III mode mixity. The mode mixities, ψ, are defined as:

Table 1
Material properties for graphite/epoxy laminate

$E_{11} = 144.23$ GPa, $E_{22} = 9.65$ GPa, $E_{33} = 9.65$ GPa
$G_{12} = 4.14$ GPa, $G_{13} = 4.14$ GPa, $G_{23} = 3.45$ GPa
$v_{12} = 0.301$, $v_{13} = 0.301$, $v_{23} = 0.49$
$\alpha_{11} = 0.88$ μm/m K, $\alpha_{22} = 31.0$ μm/m K, $\alpha_{33} = 31.0$ μm/m K
$K_{11} = 4.48$ W/m K, $K_{22} = 3.21$ W/m K, $K_{33} = 3.21$ W/m K

11 is the longitudinal direction (fiber direction), 33 the transverse, and 22 the normal direction.

Table 2
Convergence of SIFs for a crack in a homogeneous anisotropic half plane

	Number of integration points, N						
	10	50	100	150	200	250	300
K_{II}	4.86e−001	5.46e−001	5.51e−001	5.53e−001	5.53e−001	5.53e−001	5.53e−001
K_I	3.02e−002	3.21e−002	3.21e−002	3.21e−002	3.21e−002	3.21e−002	3.21e−002

Material: 0°; $x_{20} = 10$ mm; $a = 1$ mm; $q_0 = 1$ W/m K; data are in $m^{1/2}$ Pa.

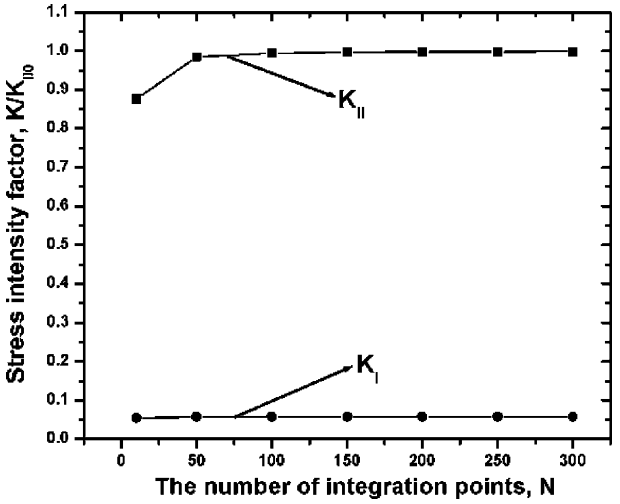

Fig. 3. The convergence of the mixed-mode stress intensity factors for 0° material.

Table 3
Comparison of the numerical method with the analytical results for the limit of infinite plane

	The numerical method			The analytical method (Sturla and Barber, 1988a, 1988b)		
	K_{II}	K_I	K_{III}	K_{II}	K_I	K_{III}
0°	0.551	3.23e−010	5.68e−015	0.5548	0	0
45°	0.364	6.26e−011	0.0849	0.36614	0	0.085459
90°	0.28018	−5.84e−016	2.35e−012	0.28018	0	0

To simulate an infinite plane, x_{20} was set very large, $x_{20} = 10^{10}$ mm; $a = 1$ mm; $q_0 = 1$ W/m K; N (number of integration points) = 100. Data are in $m^{1/2}$ Pa.

$$\psi_{II} = \arctan\left(\frac{K_{II}}{K_I}\right); \qquad \psi_{III} = \arctan\left(\frac{K_{III}}{K_I}\right). \tag{3.1}$$

It can be seen from Fig. 4a–c that the mixed-mode SIFs increase linearly with the external heat flux q_0; the ply angle of the lamina influences the rate of increase. For the Mode-II SIF, the 0° material gives the highest rate of increase, the 90° gives the lowest rate of increase and the 45° material is between; For the Mode-I SIF, the 0° material gives the highest rate of increase, the 45° material gives the lowest rate of increase and the 90° material is between. Fig. 4d and e give the Mode-II and Mode-III mode mixities, which

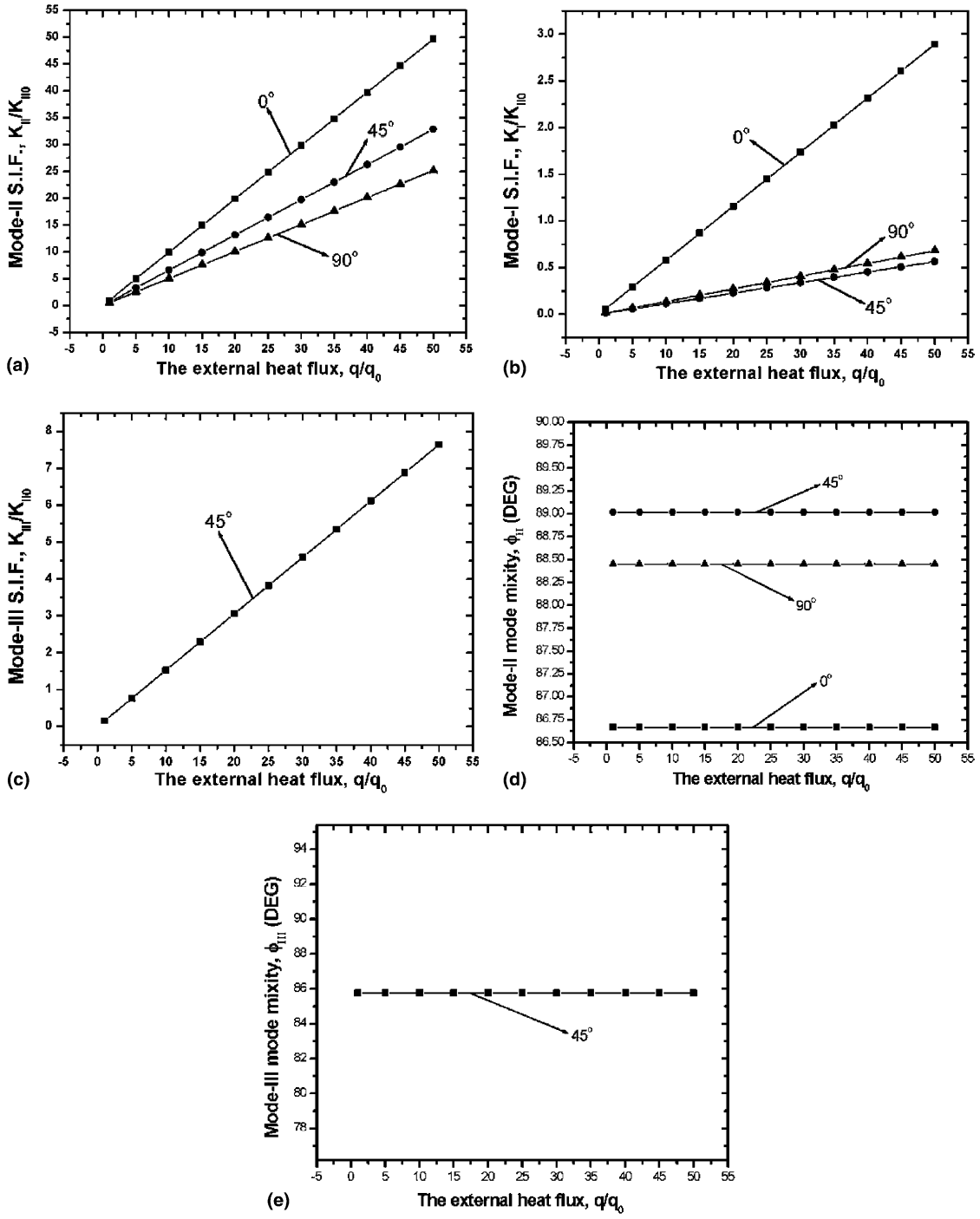

Fig. 4. SIFs and mode mixities for the half-plane crack as a function of the external heat flux: (a) Mode-II SIF, (b) Mode-I SIF, (c) Mode-III SIF, (d) Mode-II mixity, (e) Mode-III mixity.

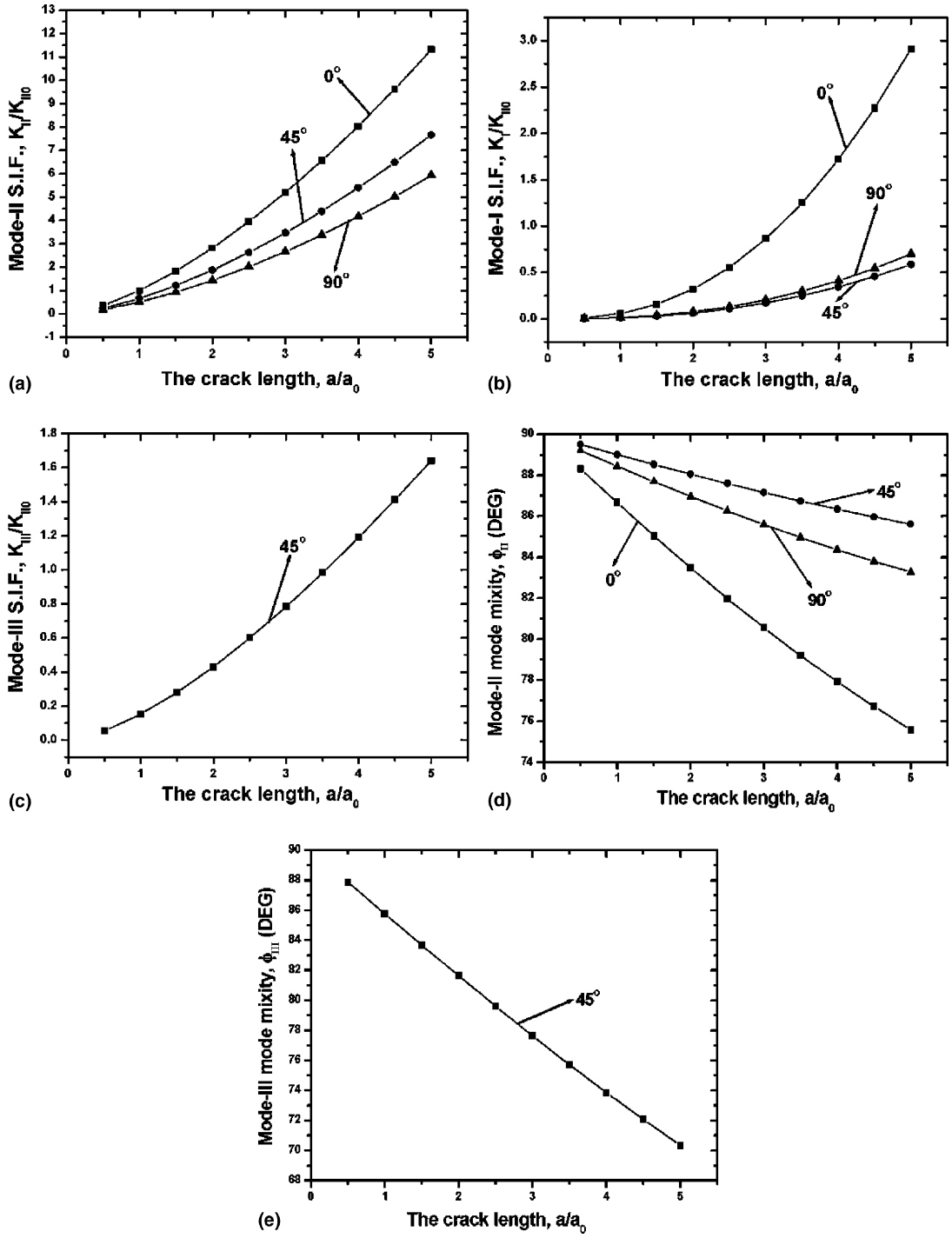

Fig. 5. SIFs and mode mixities for the half-plane crack as a function of crack length: (a) Mode-II SIF, (b) Mode-I SIF, (c) Mode-III SIF, (d) Mode-II mixity, (e) Mode-III mixity.

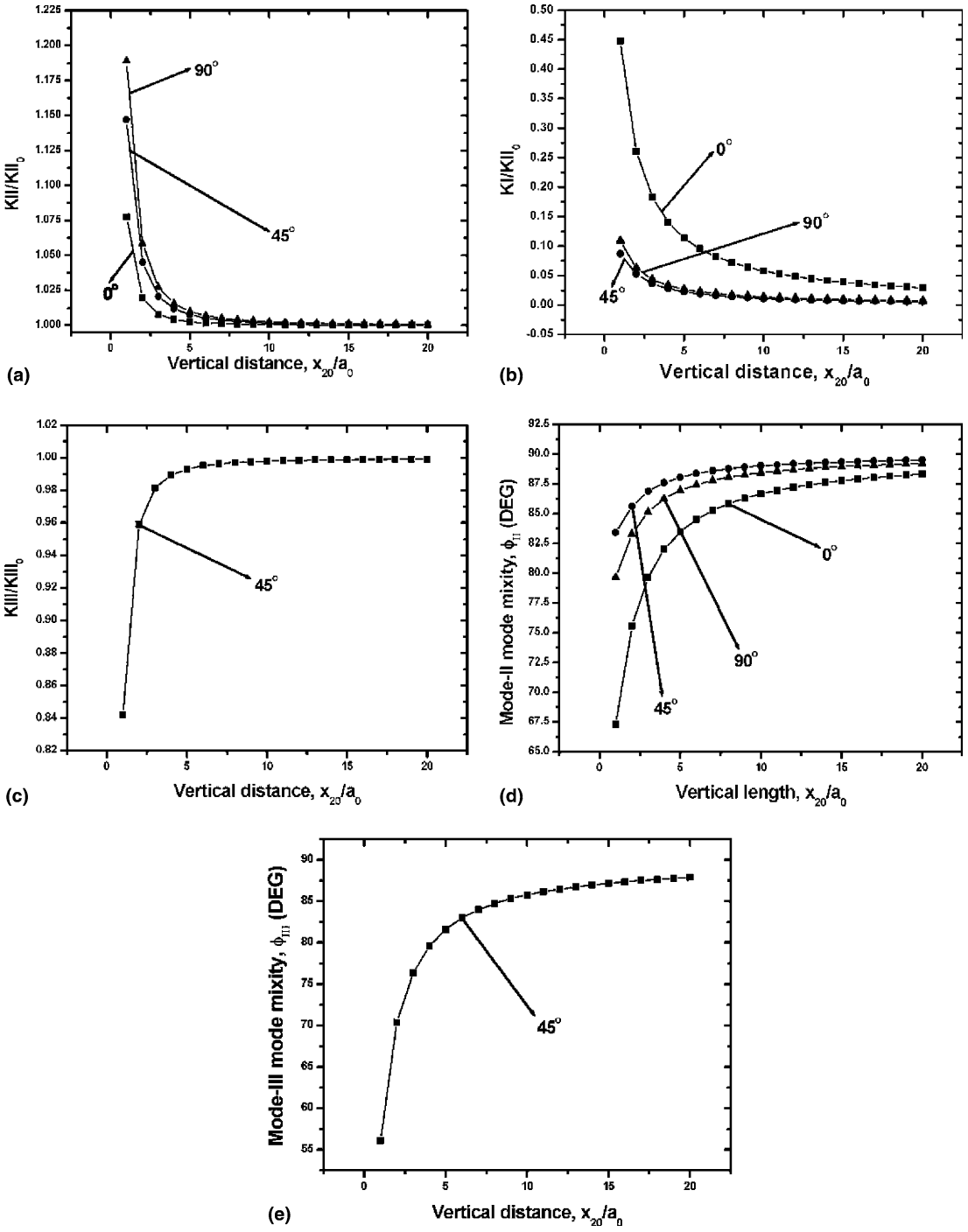

Fig. 6. (a) SIFs for half-plane cracks, normalized with the infinite plane case, and corresponding mode mixities, vs distance from the free boundary; x_{20} is the vertical distance between the crack tip and the free boundary: (a) Mode-II SIF, (b) Mode-I SIF, (c) Mode-III SIF, (d) Mode-II mixity, (e) Mode-III mixity.

are constant as the external heat flux q_0 increases; this means that the external heat does not influence the ratio between Mode-I and Mode-II or Mode-III components. This conclusion of the half plane configuration is the same with of that of the infinite plane.

Fig. 5a–e display the influence of the crack length to the three modes of stress intensity factors and mode mixities. The crack is located at $x_{20} = 1$ and the external heat flux is $q_0 = 1.0$. It can be seen in these figures that the ply angle of the lamina affects the three modes of stress intensity factors. Fig. 5a–c give the stress intensity factors for the half plane cracks with different ply angles, as a function of crack length. Clearly, the three modes of stress intensity factor increase with the length of cracks. The 0° material has the highest Mode-I and Mode-II stress intensity factors, the 90° material gives the lowest K_{II} and the 45° material gives the lowest K_I. The ply angle influences the mode mixity ψ as well. The non-zero mode mixity indicates cracks are prone to propagate away from the original crack orientation. For all composite laminae discussed here, the mode mixities decrease with the crack length; a comparison of the results shows that for the 0° material, ψ_{II} decreases faster with the crack length than the other orientations.

The effect of the free boundary on the stress intensity factors is studied also and the results are shown in Fig. 6a–e. We denote the distance between the crack and the free boundary by x_{20}. In Fig. 6a, we denote K_{II0} the Mode-II stress intensity factor of the crack in an infinite plane. It can be seen that K_{II} decreases as x_{20} increases for all of the three materials; as x_{20} is large enough, K_{II} converges to K_{II0}, which means the influence of the boundary on K_{II} vanishes. In Fig. 6b, we see K_I decreases as x_{20} increases; As the distance is large enough, K_I approaches almost zero, which converges with the results of the infinite plane. The Mode-II mode mixity, ψ_{II}, is studied in Fig. 6d and ψ_{II} increases as x_{20} increases as well, which means that for mixed-mode stress intensity factors, the effect of the Mode-II stress intensity factor component compared with the K_I increases as the crack moves away from the boundary. In Fig. 6c, it can be seen that the K_{III} for the 45° material increases as x_{20} increases (where K_{III0} is the Mode-III stress intensity factor of the crack in an infinite plane). As x_{20} is large enough, K_{III} converges to K_{III0}. The Mode-III mode mixity ψ_{III} is shown in Fig. 6e, and ψ_{III} increases as x_{20} increases, which means that, as far as the mixed-mode stress intensity factors, the effect of K_{III} component compared with K_I component increases as the vertical distance x_{20} between the free boundary and the crack increases. From the Fig. 6e and d, it can be seen that all mode mixities increase with the vertical distance x_{20} increasing, since for the infinite configuration, the Mode-I stress intensity factor disappears for all three materials.

It should be noted that the selected geometry and thermal loading in the paper are very basic and simple, but based on this fundamental solution, the problem for the more practical finite domain can be solved as a direct extension of this solution, provided the anisotropic material is elastic and superimposition is valid. For example, the geometry of a dislocation in the more practical finite strip geometry can be decomposed into two configurations: the first one is a single dislocation located in the bi-material half-plane; the second geometry is also the half-plane with one dislocation array located along the boundary of the strip and the density of the dislocation array is determined in such a way that the corresponding stress and thermal boundary conditions are satisfied. Finally, the technique can be developed as the dislocation-based boundary element method which the potential to solve crack problem in anisotropic structures with arbitrary geometries and loadings. We plan to work in the future along the line of these extensions of the present work.

4. Conclusions

Dislocation solutions for a fully-open crack in a general anisotropic half plane under uniform heat flux have been obtained. The convergence and accuracy of the results for the half plane are verified with the analytical results for an infinite plane by setting the free boundary infinite. The method presented is applied to calculate the mixed-mode stress intensity factors. Based on the results, the following conclusions can be

drawn: (1) For a general anisotropic material, the ply angle affects the mixed mode stress intensity factors. (2) For the half plane with free boundary parallel to the crack surface, the external heat flux can affect the mixed-mode stress intensity factors, which increase linearly with the heat flux q_0, but q_0 does not seem to influence the mode mixity. (3) Regarding the effect of crack length, the three SIF components increase as the length of the crack increases; also, the mode mixities decrease with the crack length increasing for all three materials studied. (4) The distance between the crack and the free boundary influences the mixed mode stress intensity factors. For all three materials with different ply angles studied, the Mode-I and Mode-II stress intensity factors, decrease, but the Mode-III SIF increases with the increasing distance between crack and free boundary; also, the mode mixities increase as the vertical distance increases.

Acknowledgements

The financial support of the Office of Naval Research, Grant N00014-03-1-0189, and the interest and encouragement of the Grant Monitors, Dr. Patrick C. Potter and Dr. Luise Couchman is gratefully acknowledged.

References

Atkinson, C., Clements, D.L., 1997. On some crack problems in anisotropic thermoelasticity. Int. J. Solids Struct. 12, 855–864.

Atkinson, C., Eftaxiopoulos, D.A., 1991. Interaction between a crack and a free or welded boundary in media with arbitrary anisotropy. Int. J. Fract. 50, 159–182.

Civelek, M.B., Erdogan, F., 1982. Crack problems for a rectangle plate and an infinite strip. Int. J. Fract. 19, 139–159.

Clements, D.L., 1973. Thermal stress in anisotropic elastic half-space. SIAM J. Appl. Math. 23 (3), 332–337.

Clements, D.L., Toy, G.D., 1976. Two contact problems in anisotropic thermoelasticity. J. Elasticity 6 (2), 137–147.

Eshelby, J.D., Read, W.T., Shockley, W., 1953. Anisotropic elasticity with applications to dislocation theory. Acta Meta. 1, 251–259.

Hills, D.A., Kelly, P.A., Dai, D.N., Korsunsky, A.M., 1996. Solution of Crack Problems; the Distributed Dislocation Technique. Kluwer Academic Publishers, UK.

Huang, H., Kardomateas, G.A., 2001. Mixed-mode stress intensity factors for cracks located at or parallel the interface in bi-material half planes. Int. J. Solids Struct. 38, 3719–3734.

Kim, H.S., Chattopadhyay, A., Nam, C., 2002. Implementation of a coupled thermo-piezoelectric-mechanical model in the LQG controller design for smart composite shells. J. Intel. Mater. System Struct. 43 (11), 713–724.

Sekine, H., 1977. Thermal stress near tips of an insulated line crack in a semi-infinite medium under uniform heat flow. Eng. Fract. Mech. 9, 499–507.

Stroh, A.N., 1958. Dislocations and cracks in anisotropic elasticity. Philos. Mag. 3, 625–646.

Sturla, F.A., Barber, J.R., 1988a. Thermoelastic Green's function for plane problems in general anisotropy. J. Appl. Mech., Trans. ASME 55, 245–247.

Sturla, F.A., Barber, J.R., 1988b. Thermal stress due to a plane crack in general anisotropic material. J. Appl. Mech., Trans. ASME 55, 372–376.

Suo, Z., 1990. Delamination specimens for orthotropic materials. J. Appl. Mech. 57, 627–634.

Suo, Z., Hutchinson, J.W., 1990. Interface crack between two elastic layers. Int. J. Fract. 43, 1–18.

Ting, T., 1986. Explicit solution and invariance of the singularities at an interface crack in anisotropic composites. Int. J. Solids Struct. 22 (9), 965–983.

Tsai, Y.M., 1983. Thermal stress in a transversely isotropic medium containing a penny-shaped crack. J. Appl. Mech., Trans. ASME 50 (1), 24–28.

Tsai, Y.M., 1984. Orthotropic thermoelastic problem of uniform heat flow distributed by a central crack. J. Compos. Mater. 18 (2), 122–131.